JPET Fast Forward. Published on April 22, 2019 as DOI: 10.1124/jpet.118.255984
This article has not been copyedited and formatted. The final version may differ from this version.

JPET #255984

The mitoNEET ligand NL-1 mediates anti-leukemic activity in drug resistant B-cell acute lymphoblastic leukemia.

Werner J Geldenhuys[#], Rajesh R Nair[#], Debbie Piktel, Karen H Martin and Laura F Gibson

Department of Pharmaceutical Sciences, School of Pharmacy, West Virginia University, Morgantown, West Virginia, United States (W.J.G.)

Department of Microbiology, Immunology and Cell Biology, School of Medicine, West Virginia University, Morgantown, West Virginia, United States (R.R.N, K.H.M., L.F.G.)

Robert C. Byrd Health Sciences Center, West Virginia University, Morgantown, West Virginia, United States. (W.J.G., R.R.N., D.P., K.H.M., L.F.G.)

WVU Cancer Institute, West Virginia University, Morgantown, West Virginia, United States. (W.J.G., K.H.M., L.F.G.)

Running Title Page

Anti-cancer activity of NL-1 in leukemia

Address corresponding to: Laura F. Gibson, PO Box 9104, 64 Medical Center Drive, West Virginia University, Morgantown, WV 26506, TEL: 304-293-7206, Email: lgibson@hsc.wvu.edu

[#] Equal contribution

Number of text pages: 37

Number of tables: 0

Number of figures: 7

Number of supplementary figures: 0

Number of references: 49

Number of words in Abstract: 248

Number of words in Introduction: 540

Number of words in Discussion: 1463

Non-standard abbreviations

CQ, chloroquine; ALL, acute lymphoblastic leukemia

Recommended section assignment:

Drug Discovery and Translational Medicine

Abstract

Disease relapse in B-cell acute lymphoblastic leukemia (ALL), either due to development of acquired resistance after therapy or because of *de novo* resistance, remains a therapeutic challenge. In the present study, we have developed a cytarabine (Ara-C) resistant REH cell line (REH/Ara-C) as a chemoresistance model. REH/Ara-C (a) was not cross-resistant to vincristine or methotrexate; (b) showed a similar proliferation rate and cell surface marker expression as parental REH; (c) demonstrated decreased chemotaxis towards bone marrow stromal cells (BMSC); and (iv) expressed higher transcript levels of cytidine deaminase (*CDA*) and mitoNEET (*CISD1*) than the parental REH cell line. Based on these findings, we tested NL-1, a mitoNEET inhibitor, which induced a concentration-dependent decrease in cell viability with a comparable IC_{50} in REH and REH/Ara-C. Furthermore, NL-1 decreased cell viability in six different ALL cell lines and showed inhibitory activity in a hemosphere assay. NL-1 also impaired the migratory ability of leukemic cells, irrespective of the chemoattractant used, in a chemotaxis assay. More importantly, NL-1 showed specific activity in inducing death in a drug resistant population of leukemic cells within a co-culture model that mimicked the acquired resistance and *de novo* resistance observed in the BM of relapsed patients. Subsequent studies indicated that NL-1 mediates autophagy, and inhibition of autophagy partially decreased NL-1-induced tumor cell death. Finally, NL-1 showed anti-leukemic activity in an *in vivo* mouse ALL model. Taken together, our study demonstrates that mitoNEET has potential as a novel anti-leukemic drug target in treatment refractory or relapsed ALL.

Introduction

In B-cell acute lymphoblastic leukemia (ALL) patients, there is a positive correlation between drug resistance and poor prognostic clinical outcome, independent of age, gender and initial leukemic burden (Pieters et al., 1991; Kaspers et al., 1997). Emergence of drug resistance after chemotherapy is a common phenomenon in newly relapsed ALL patients and unfortunately, the drug-resistance profile worsens with subsequent relapse (Klumper et al., 1995; Pogorzala et al., 2015). Additionally, throughout disease progression, leukemic cells are constantly modifying their bone marrow (BM) microenvironment to form a leukemic niche, which affords *de novo* chemoresistance (Colmone et al., 2008). This *de novo* resistance leads to survival of leukemic cells after therapy, and the residual surviving cell number is a measure of minimal residual disease (MRD). Importantly, MRD is correlated with a poor prognosis in patients (Stow et al., 2010).

In order to study drug resistance in leukemic cells, we previously developed an *in vitro* co-culture model consisting of human-derived ALL cells cultured in the presence of either primary human bone marrow stromal cells (BMSC) or primary human osteoblasts (HOB) (Moses et al., 2016b). Using this model, we developed a protocol to isolate and characterize a subset of phase dim (PD) leukemic cells that buried under the BM-derived adherent layer (Slone et al., 2016b). PD cells share the characteristics typical of relapsed/refractory leukemic cells, in that they are quiescent and resistant to chemotherapy, had impaired microRNA biogenesis, and relevant to the current study, manifested altered mitochondrial metabolism (Moses et al., 2016a; Moses et al., 2016b; Slone et al., 2016a). This drug-resistant phenotype was context-dependent and transient, as removing the PD cells from the co-culture restored their sensitivity to chemotherapy treatment. In the present study we have developed a cytarabine-resistant REH cell line (REH/Ara-C) and co-

cultured it with BMSC or HOB to mimic both the acquired and *de novo* drug resistant phenotype generally found in the BM of relapsed ALL patients.

Central to the rationale of this investigation is work by others in which mitochondrial dysfunction has been shown to be associated with chemoresistance and has been targeted as a strategy for anti-cancer therapy (Neuzil et al., 2013). Evasion of programmed cell death is one of the major mechanisms of drug resistance and cancer progression (Hanahan and Weinberg, 2011), and targeting mitochondrial function may be a therapeutic option in targeting this population of cells (Fu et al., 2017; Kuntz et al., 2017).

MitoNEET (*CISD1*) is a mitochondrial outer membrane protein that plays a critical role in maintaining mitochondrial homeostasis and is frequently overexpressed in cancer (Bai et al., 2015). This 2Fe-2S cluster-containing protein was first discovered as a secondary target for the anti-diabetic drug pioglitazone (Colca et al., 2004). In the present study we have utilized a small molecule ligand of mitoNEET called NL-1 which was derived from pioglitazone (Geldenhuys et al., 2010) and demonstrated its anti-leukemic activity in both acquired and *de novo* drug resistant cells (Fig. 1). NL-1, pioglitazone and rosiglitazone belong to the glitazones or thiazolidinedione (TZD) class of compounds. Additionally, we show that NL-1-mediated death in leukemic cells requires the activation of the autophagic pathway. These results led us to propose the use of NL-1 for the treatment of relapsed ALL leveraging the vulnerability of the mitochondria as a therapeutic strategy.

Materials and Methods

Cell cultures. Nine human B-cell ALL cell lines were purchased from ATCC or DSMZ. SUP-B15 (CRL-1929), TOM-1 (ACC 578) and JM1 (CRL-10423) cells were maintained in RPMI 1640 containing 10% FBS, 0.05 mM β-mercaptoethanol and 1x streptomycin/penicillin. REH (CRL-8286), NALM-1 (CRL-1567), NALM-6 (ACC 128), BV-173 (ACC 20), RS4;11 (CRL-1873) and SD-1 (ACC 366) were maintained in RPMI 1640 containing 10% FBS and 1x streptomycin/penicillin. Primary $CD3^+$ T cells, $CD19^+$ B cells, peripheral blood mononuclear cells (PBMC) and bone marrow mononuclear cells (BMMC) were purchased from AllCells (Allcells.com) and maintained in Lymphocyte Growth Medium-3 (Lonza, Cat No: CC-3211) containing 10% FBS and 1x streptomycin/penicillin. Human osteoblasts (HOB) were purchased from PromoCell (Cat No: C-12720, Heidelberg, Germany) and cultured according to the vendor's recommendations.

A chemotherapy-resistant REH ALL cell line (REH/Ara-C) was developed by exposing REH cells to increasing concentrations of Ara-C starting at 0.2 μM. Following a one week period, if cell viability of the Ara-C treated culture was determined to be greater than 70%, the concentration of Ara-C was increased by 0.1 μM. The resulting REH/Ara-C cell line was maintained in growth media containing 1 μM Ara-C, and all experiments utilizing REH/Ara-C cells were carried out following 48 hours of exposure to 1 μM Ara-C.

De-identified primary BMSC were provided by the WVU Cancer Institute Biospecimen Processing Core and the WVU Pathology Laboratory Tissue Bank. The ALL cell lines used in the

current study were authenticated by short tandem repeat (STR) analysis (University of Arizona Genetics Core, Tucson, AZ) and maintained in 6% CO_2 in normoxia at 37 $^{\circ}$C.

Cell proliferation assays. ALL cell lines were plated at 5 x 10^4 cells/well in a 96 well plate. Following treatment with chemotherapy, pharmacologic inhibitors or NL-1**,** viable cells were quantitated using a Cell Counting Kit-8 (Dojindo Molecular Technology Inc.) according to manufacturer's instructions.

Cell surface expression analysis. Cell surface proteins were stained with fluorochrome-conjugated antibodies to CD19 (PerCP, #34072), CD34 (PE, #550761), CD38 (APC, #34072), CD44 (FITC, #555478) and CD45 (PE-Cy5, #555484) in staining buffer (PBS + 10% FBS) for 1 hour at RT. Cells were washed with PBS, fixed with 1% paraformaldehyde and resuspended in PBS for analysis of mean fluorescence intensity by flow cytometry (BD LSR Fortessa). Fluorochrome-conjugated isotype controls were used for measuring non-specific binding.

Chemotaxis assay. BMSC or HOB were plated at 90% confluency in 24-well transwell plates (Costar, Cat No.3421). After overnight incubation, untreated ALL cells or NL-1 [60 μM] pre-treated cells (1 hour pre-treatment) were plated at 1.5 x 10^5 cells in the top of the transwell insert. The cells were allowed to migrate toward adherent layers for 4 hours. Migrated leukemic cells were collected, fixed by 2% paraformaldehyde and counted using flow cytometry. SDF-1 (100 ng/ml) served as the positive control for the chemoattractant and media alone as the negative control.

Real-time quantitative reverse transcriptase polymerase chain reaction (qRT-PCR). REH and REH/Ara-C cells were plated at 1 x 10^6 cells/ml and cultured overnight, following which the cells were pelleted and processed for RNA extraction using an RNeasy kit (Qiagen, Cat No. 74104) according to the manufacturer's instruction. RNA (50 ng) was then amplified by real time PCR using the Power SYBR Green RNA-to-C_T 1-Step kit (ThermoFisher Scientific, Cat No. 4389986) with primers specific for CDA (# VHPS-1708), DCK (#VHPS-2471), RRM1 (#VHPS-8020) and ACTB (VHPS-110) purchased from RealTimePrimers.com and primers for SCL19A1(FWD 5'-GAA CCC GTT TGA GCT CGG TA-3'and REV 5'-GCT GCG ATC CAT TCA ACT CG-3') and CISD1(FWD 5'-CCT CCT GGT GTC AGC AAG CT-3' and REV 5'-CCC GAG AGT CAC TGG TTC ACA-3') purchased from Integrated DNA Technologies. The gene expression in REH and REH/Ara-C was normalized to ACTB and the fold difference in gene expression between the two cells lines was subsequently analyzed.

Hemosphere assay. SD1 leukemic cells were plated at 1 x 10^5 cells/well in a 96 well plate and incubated for 4 days to allow sphere formation. Following confirmation of spheroids in culture by light microscopy, the cells were treated with 60 μM NL-1 for 72 hours. At the end of the treatment, the resultant spheroids were counted via microscopy and the images were captured (Leica DMIL LED microscope/camera). Cells were collected at the end of the study and counted with Trypan Blue (0.4% v/v) to determine number of live cells.

Co-culture study. Co-culture conditions have been previously described (Slone et al., 2016b). Briefly, 1 x 10^6 REH or REH/Ara-C cells were seeded on either BMSC or HOB adherent layers and maintained in 5% O_2. The co-culture was fed every 4 days, and on the 9^{th} day the co-culture

was treated with 60 μM NL-1 for 72 hours. Following exposure, ALL cells that were in suspension were collected (suspended cells; S). The ALL cells that were buried under the adherent layer were trypsinized and separated from BMSC or HOB by size exclusion using Sephadex G-10 columns. These buried ALL cells were designated as phase dim cells (PD) and have been previously described to share relevant characteristics with cells that contribute to treatment resistant MRD (Moses et al., 2016a; Slone et al., 2016a).

Autophagy detection assay. REH cells were plated at 1 x 10^6 cells/ml and then treated with 5 μM chloroquine for 1 hour. Following chloroquine treatment, the cells were exposed to 60 μM NL-1 for 6 hours. At the end of the treatment, the autophagic flux was measured using a CYTO-ID Autophagy detection kit 2.0 (Enzo Life Sciences, Cat No. ENZ-KIT 175) according the manufacturer's instructions. Briefly, treated cells were washed with 1x assay buffer and resuspended in CYTO-ID green stain solution for 30 min at 37 ºC. Following incubation, the cells were thoroughly washed and cell density was adjusted to 5 x 10^4 cells/ml. 100 μl of this cell suspension was plated in triplicate in a 96 well plate and the fluorescence intensity was measured with a Biotek plate reader Synergy HT using a FITC filter (Excitation 480 nm, Emission 530 nm).

Cell death assay. Primary immune cells were plated at 1 x 10^6 cells/ml in 24 well plates. The cells were treated with 60 μM NL-1 for 24 hours and then stained using a LIVE/DEAD Fixable Dead Cell Stain Kit (ThermoFisher Scientific) following the manufacturer's instructions. The number of dead cells were then analyzed using flow cytometry.

***In vivo* study.** All animal procedures were reviewed and approved by the WVU Institutional Animal Care and Use Committee. Ten 6-8 month old female NOD.Cg-*Prkdc*^{scid} *Il2rg*^{tm1Wjl}/SzJ (NSG) mice were IV-injected with 1 x 10^6 luciferase-expressing TOM-1 ALL cells. Two days post-injection, the mice were injected with luciferin and the tumor burden was analyzed using an IVIS SpectrumCT. After confirmation of tumor engraftment, the mice were randomized into two groups of five mice each and treated with 1 mg/kg NL-1 or vehicle-control, IP, for five consecutive days. Tumor burden was monitored weekly using IVIS imaging. The study was terminated when the control mice showed signs of morbidity due to high tumor burden.

Statistical analysis. *In vitro* experiments were performed in triplicate in at least three independent experiments, unless otherwise stated. For studies consisting of more than two treatment groups, statistical significance between groups was determined using one-way ANOVA followed by a post-hoc Tukey's test. For the chemotaxis assay, two-way ANOVA followed by a post hoc Sidak's multiple comparison test was used to determine statistical significance. For the *in vivo* study, an unpaired one-tailed t test was performed to determine the statistical significance between the NL-1 treated and control vehicle-treated mice. Data are shown as mean ± SEM and $p<0.05$ was considered as statistically significant.

Results

Development of a chemotherapy-resistant ALL cell line. The emergence of chemotherapy-resistant tumors presents a major clinical challenge in the long-term treatment of ALL patients. In order to generate a model to address chemotherapy-resistant disease, the REH ALL cell line was treated with increasing doses of Ara-C over the course of several months to generate a cell line that is resistant to this drug (REH/Ara-C). A dose response curve using Ara-C was performed to compare the REH/Ara-C cells to the parental REH cells. As expected, there was a dose-dependent decrease in the number of viable REH cells, with an IC_{50} of 19.5 nM; however, Ara-C had no effect on the number of viable REH/Ara-C cells, even at doses 10 times higher than the IC_{50} for the parental line (Fig. 2A). The chemotherapy resistance in the REH/Ara-C cell line was specific to that treatment, as those cells remained sensitive to other chemotherapy reagents including methotrexate (Fig. 2B) and vincristine (Fig. 2C), showing IC_{50} values comparable to the parental cell line, REH (Fig. 2D).

REH/Ara-C cell line shows increased *CISD1* levels. Further experiments were performed using the REH and REH/Ara-C cells to assess the functional or expression differences that may contribute to the differential sensitivity to chemotherapy. REH and REH/Ara-C had similar cell proliferation rates; the modest difference noted at day 4 was not statistically significant (Fig. 3A). Analysis of cell surface receptors demonstrated that CD19, CD34, CD38, CD44 and CD45 were present at the same levels in both REH and REH/Ara-C cell lines (Fig. 3B). Interestingly, the chemotactic ability of the REH/Ara-C cells to migrate toward BMSC, HOB, and SDF-1 was diminished when compared to the REH parental cell line. However, no difference was observed between the two cell lines when media was used as chemoattractant (Fig. 3C). Gene expression

JPET Fast Forward. Published on April 22, 2019 as DOI: 10.1124/jpet.118.255984
This article has not been copyedited and formatted. The final version may differ from this version.

analysis showed a 3 fold increase in the level of cytidine deaminase transcripts (*CDA*) and a 1.7 fold increase in mitoNEET (*CISD1*) transcripts (Fig. 3D); however, deoxycytidine kinase (*DCK*), ribonuclease reductase M1 polypeptide (*RRM1*) and solute carrier family 19 (folate transporter) member 1 (*SCL19A1*) transcripts were comparable to the parental cell line.

NL-1 shows anti-cancer activity in ALL cell lines. Based on the increased expression of mitoNEET in the drug-resistant cell line, we tested the activity of a mitoNEET ligand, NL-1. Treatment with NL-1 reduced the number of viable cells in both REH and REH/Ara-C cell lines, in a concentration-dependent manner (Fig. 4A). The IC_{50} of NL-1 was comparable in REH (47.35 ± 7.7 μM) and REH/Ara-C cells (56.26 ± 8.8 μM) (Fig. 4B). Furthermore, NL-1 successfully decreased the number of viable cells in a concentration-dependent manner in six additional ALL cell lines (Fig. 4C). SUPB15 was the most sensitive to NL-1 with an IC_{50} of 29.48 ± 10.66 μM, and NALM6 demonstrated the most resistance to NL-1 with an IC_{50} of 94.26 ± 2.60 μM (Fig. 4D). In contrast, TOM1, BV173, NALM1 and JM1 all had similar IC_{50} values of around 60 μM for NL-1 (Fig. 4D). Furthermore, we utilized SD1 ALL cells to form hemospheres for evaluation of NL-1 in a model of tumor "stem cell like" behavior. In contrast to the REH cells, SD1 cells will form hemospheres, suited for this experimental design to identify compounds, which will target this cell population. SD1 cells formed 10-15 spheroids/well. After the spheroids formed, they were treated with NL-1. NL-1 treatment consistently reduced the size and the number of pre-formed SD1 spheroids (Fig. 5A-B). Additionally, we found that both the number of live cells (Fig. 5C) and the % viability (Fig. 5D) of the cells was reduced when treated with NL-1.

NL-1 impairs chemotaxis in ALL cells. Soluble factor gradients driving chemotaxis play an important role in leukemic niche development (Mohle et al., 2000; Colmone et al., 2008). Our initial studies showed that parental REH and drug resistant REH/Ara-C both had comparable chemotaxis profiles with REH/Ara-C showing only a modest decrease in its migratory capacity towards BMSC. NL-1 pretreatment inhibited the chemotactic ability of both REH (Fig. 5E) and REH/Ara-C (Fig. 5F) cells to migrate towards multiple chemoattractants. This inhibitory NL-1 activity was most pronounced in REH and REH/Ara-C cells migrating towards the BMSC, although there were also significant differences in all of the conditions. The cells treated with NL-1 showed a dose-dependent decrease in chemotaxis both in the REH (Fig. 5 G) and the REH/Ara-C cells (Fig. 5H).

NL-1 induces death in the drug resistant phase dim (PD) ALL cell population. In order to model the bone marrow microenvironment which can provide a site of sanctuary for leukemia, our lab has previously developed a co-culture model where ALL cells are grown with either primary human BMSC or HOB. The leukemia cells form three populations in the co-culture: those floating in suspension (S), those loosely adhered to the top of the stromal cell layer, and the cells that bury underneath the stromal cells (PD). The PD leukemic cells consistently show increased resistance to a variety of chemotherapies. In order to determine whether NL-1 could affect cells that are protected by both bone marrow microenvironment cues as well as acquired drug resistance, NL-1 was tested in co-cultures including either REH or REH/Ara-C cells. Treatment of BMSC and HOB co-cultures with NL-1 decreased the number of live cells recovered from the S and PD populations (Fig. 6A and C) and decreased viability of the PD population (Fig. 6B and D), where the number of live cells were determined with Trypan Blue live staining In these conditions, the

suspension cells (S) showed a small but significant decrease in the number of live cells in the REH/Ara-C suspension (S) cells, but the viability was not decreased.

NL-1-mediated induction of autophagy. MitoNEET has been shown to play a role in mitophagy during autophagy (Lazarou et al., 2013). To determine if NL-1 modulates autophagic flux in ALL cells, we used a fluorescent dye that specifically labels autophagososomes. Treatment with NL-1 nearly increased the fluorescence intensity compared to untreated cells, indicating an increase in autophagy (Fig. 6E). The specificity of the assay was confirmed by pre-treating the cells with chloroquine, an inhibitor of autophagy. Treating ALL cells with chloroquine before the addition of NL-1 reduced the increase in fluorescence slightly (Fig. 6E). To investigate if autophagy is critical in NL-1-mediated induction of death in leukemic cells, we pretreated cells with increasing doses of chloroquine followed by NL-1 and then analyzed cell viability. Treatment with NL-1 by itself caused death in REH cells (Fig. 6F). Pretreatment with 1 and 5 μM chloroquine to inhibit autophagy reduced the amount of NL-1-mediated cell death significantly in both the REH and REH\Ara-C cells (Fig. 6F). We repeated this pharmacological inhibitory study in TOM1 and observed a similar reduction in NL-1-mediated death (supplementary data 1).

NL-1 has anti-leukemic activity *in vivo.* In order to determine whether NL-1 would negatively affect the viability of other hematopoietic cells, we treated primary immune cells with NL-1 and found that NL-1 did not substantially decrease cellular viability in those cells (Fig. 7A). NL-1 caused the highest increase in death in CD3 T cells (12.00 ± 0.66 %) followed by PBMC (11.00 ± 5.00 %) then CD19 B cells (7.57 ± 5.44 %) and finally BMMC (2.00 ± 1.00 %). To determine whether NL-1 would affect leukemic cell growth *in vivo*, we evaluated NL-1 in a pilot study with

a single dose of NL-1, where we injected TOM1 ALL cells expressing luciferase into NSG mice. After confirming leukemic cell engraftment by IVIS luminescent imaging, the mice were treated with 10 mg/kg NL-1 every day for 5 days. The dose was based on our previous pharmacokinetic study (Pedada et al., 2014). Out of the ten mice, one control mouse did not show tumor progression after engraftment and was not included in the study. On day 14 post-injection, the NL-1 treated group showed significantly lower tumor burden than the control vehicle treated group (Fig. 7B).

Discussion

In the present study, we have developed an Ara-C resistant leukemic cell line (REH/Ara-C) to model the development of chemotherapy resistance observed in patients with ALL. REH/Ara-C cells overexpress *CDA* and *CISD1* (mitoNEET protein) transcripts. This overexpression did not result in cross-resistance to methotrexate or vincristine but was associated with altered migratory capacity toward BMSC, HOB, and SDF-1. Targeting the mitochondrial protein mitoNEET (CISD1) with NL-1 decreased the viability in several ALL cell lines with comparable IC_{50}. Moreover, NL-1 efficiently disrupted pre-formed spheroids in a hemosphere assay and was able to inhibit the chemotaxis of both parental REH and REH/Ara-C cell lines. More importantly, NL-1 was able to specifically decrease the viability of REH/Ara-C in a co-culture model that models the combination of acquired and *de novo* drug resistance found in relapsed patients. The NL-1-mediated cell death was attributed to its ability in part to induce autophagy as pretreatment with the autophagy inhibitor chloroquine was able to reduce NL-1 mediated cell death. Finally, NL-1 was non-toxic to normal immune cells and showed significant anti-leukemic activity in a pilot study using a mouse model of ALL.

B-cell ALL relapsed patients are treated with a combination of chemotherapy and hematopoietic stem cell transplantation (Eckert et al., 2013). The anti-tumor effect of Ara-C varies widely in the clinic and is related to genetic variation in the key genes involved in the uptake, activation and metabolism of Ara-C within the tumor cells (Lamba, 2009). *SCL19A1* is a folate transporter that is responsible for the uptake of Ara-C and has been shown to be down-regulated in Ara-C resistant cells (Gati et al., 1997). Once inside the cells, Ara-C is activated by

deoxycytidylate deaminase (*DCK*) and its expression has been reported to be decreased in relapsed patients (Kakihara et al., 1998). Ara-C is inactivated by cytidine deaminase (*CDA*) which has been shown to be upregulated in drug resistant cells (Schroder et al., 1998). Finally, ribonucleotide reductase M1 (*RRM1*) catalyzes and maintains the intracellular pools of dCTP, which directly competes with activated Ara-C for incorporation within the DNA (Liliemark and Plunkett, 1986). In our study, *CDA* was upregulated in the REH/Ara-C cell line and may be the cause of resistance to Ara-C. As the upregulated CDA has little role to play in modulation of vincristine and methotrexate activity, not surprisingly, these drugs showed similar sensitivity in REH/Ara-C compared to REH cells. This lack of cross resistance has been previously demonstrated in T-lymphoblastic leukemia cells that were resistant to Ara-C (Cai et al., 2008). Since there are no clinical therapies available to mitigate the overexpression of *CDA*, we sought to identify a druggable target for treatment of relapsed ALL patients. Our previous studies have shown that the drug resistance phenotype is accompanied by mitochondrial dysfunction (Moses et al., 2016b). In light of this, we looked at the mitochondrial protein mitoNEET expression in REH/Ara-C cells and found it to be up-regulated in the drug resistant cells compared to parental REH cells.

MitoNEET has been previously described as being overexpressed in cancer cells of epithelial origins (Sohn et al., 2013). Specifically, constitutive overexpression of mitoNEET increases tumor size in breast cancer and conversely, knocking down the expression of mitoNEET decreased proliferation and tumor development in human breast cancer cells (Sohn et al., 2013; Tamir et al., 2015). Furthermore, a bioinformatics study of gene expression analysis has revealed that mitoNEET expression is elevated in several other solid tumors (Stelzer et al., 2011). MitoNEET is an iron-sulfur 2Fe-2S cluster protein located on the outer mitochondrial membrane, which acts as redox sensor and regulates mitochondrial bioenergetics (Mittler et al., 2018).

However, the role of mitoNEET as a potential drug target in ALL had not yet been investigated. In our studies, we have found that mitoNEET, along with *CDA*, is overexpressed in our acquired drug resistant cell line, REH/Ara-C. Overexpression in REH/Ara-C cells was not accompanied by changes in cell proliferation or cell surface receptor expression when compared to the parental cell line, REH.

Impaired apoptosis is one of the most crucial phenotypes associated with resistance to different classes of drugs in ALL (Holleman et al., 2003). Since mitochondria modulate the molecular players involved in apoptosis, targeting the same is an attractive strategy for therapy in cancer (Indran et al., 2011). Towards this goal, we have utilized a selective mitoNEET ligand, called NL-1, a derivative of the anti-diabetic drug pioglitazone (Geldenhuys et al., 2010; Geldenhuys et al., 2011). The use of NL-1 as an anti-cancer agent has not been reported, and our studies indicated that NL-1 has significant anti-leukemic activity. Our data show that NL-1 was effective in decreasing the cell viability of different ALL cell lines and had similar IC_{50} in the REH and the resistant REH/Ara-C cell lines. We had previously demonstrated the enrichment of ALL cells with overexpression of stem cell markers like SOX2 in hemospheres (Nair et al., 2018). We evaluated the effect of NL-1 in the SD1 ALL cells since these have a propensity to form hemospheres, NL-1 effectively disrupted pre-formed spheroids in a hemosphere assay, and the cells had significantly decreased viability (Zhang et al., 2015).We found it interesting that NL-1 was able to target and induce death in the Phase Dim (PD) cells of the REH/Ara-C cells in co-culture with either BMSC or HOB. This observation is very notable since the co-culture study mimics the acquired and *de novo* drug resistant phenotype associated with relapse in ALL patients (Mudry et al., 2000; Fortney et al., 2001; Moses et al., 2016b).

Previous studies have reported that suppression of mitoNEET is accompanied by mitochondrial dysfunction and accumulation of autophagosomes (Sohn et al., 2013). Conversely, overexpression of mitoNEET confers autophagic resistance and promotes tumor growth (Salem et al., 2012). Interestingly, autophagy plays a key role in ALL survival and leukemogenic transformation in the bone tumor microenvironment (Altman et al., 2011). Several drugs used in ALL therapy utilize activation of autophagy as a mechanism for inducing death in the leukemic cells. For example, glucocorticoids activate the autophagic machinery to induce death in primary ALL cells (Laane et al., 2009). Furthermore, idarubicin-mediated a cytotoxic autophagy in ALL cells that could be partially reversed by pretreating cells with pharmacologic inhibitors of autophagy (Ristic et al., 2014). Similarly, everolimus induced autophagy-mediated death, in ALL primary cell lines and in NOD/SCID mice xenografted with ALL cell lines, which could be partially reversed by genetic ablation of beclin-1, a key regulator of autophagy (Crazzolara et al., 2009; Neri et al., 2014). In the present study, NL-1 treatment in ALL cells led to increased autophagy which could be reduced by pre-treating cells with an autophagy inhibitor, chloroquine (Kimura et al., 2013). More importantly, inhibition of autophagy by the use of chloroquine also significantly reduced NL-1-mediated cell death in ALL. These studies suggest that the decrease in proliferation and increased cell death of the PD cells may in part due to involvement of the autophagic pathways. Future studies will focus on elucidating the key mechanisms important for cell death seen with NL-1 treatment.

In addition to survival, autophagy also plays a key role in chemotaxis. Specifically, repression of autophagy facilitates membrane trafficking and compartmentalization of critical proteins to aid in the directional chemotactic migration of cells (Coly et al., 2017). Chemotaxis plays a very important role in the niche development within the BM of leukemia patients (Gomez

et al., 2015). Previous studies using chemokine inhibitors like AMD3100 reduced tumor burden and increased leukemic death when used in combination with chemotherapy (Fei et al., 2010). Our group has demonstrated the utility of inhibiting chemotaxis as a mechanism for inducing death in drug resistant ALL cells (Nair et al., 2018). In the present study, NL-1 was sufficient to inhibit ALL chemotaxis, irrespective of the chemoattractant used in the study. The combination of the autophagy-induced death and chemotaxis might partially explain the *in vivo* anti-leukemic activity observed in our study. However, future studies to include evaluation of a stable cell line with impaired autophagy will be required to definitively validate this correlative observation made during our study.

In summary, we have demonstrated that targeting of mitoNEET by using the first-in-class compound NL-1, is a clinically viable strategy to consider to overcome drug resistance that is observed in relapsed/refractory ALL patients. This corroborates findings published by other groups that targeting mitochondrial respiration in ALL is a tractable therapeutic strategy (Fu et al., 2017; Kuntz et al., 2017). In addition to its anti-leukemic activity, NL-1 also showed a non-toxic profile when primary immune cells were exposed to it. NL-1 efficiently reduced viability in several ALL cell lines harboring different molecular drivers of leukemogenesis. Induction of death of leukemic cells in a co-culture model of acquired and *de novo* drug resistance indicates the promise of targeting mitoNEET in combination with the standard-of-care in the treatment of ALL.

Authorship Contributions

Participated in research design: Geldenhuys, Nair, Piktel, Martin and Gibson

Conducted experiments: Nair and Piktel.

Performed data analysis: Geldenhuys, Nair and Piktel

Wrote or contributed to the writing of the manuscript: Nair, Piktel, Martin and Gibson.

References

Altman BJ, Jacobs SR, Mason EF, Michalek RD, MacIntyre AN, Coloff JL, Ilkayeva O, Jia W, He YW and Rathmell JC (2011) Autophagy is essential to suppress cell stress and to allow BCR-Abl-mediated leukemogenesis. *Oncogene* **30**:1855-1867.

Bai F, Morcos F, Sohn YS, Darash-Yahana M, Rezende CO, Lipper CH, Paddock ML, Song L, Luo Y, Holt SH, Tamir S, Theodorakis EA, Jennings PA, Onuchic JN, Mittler R and Nechushtai R (2015) The Fe-S cluster-containing NEET proteins mitoNEET and NAF-1 as chemotherapeutic targets in breast cancer. *Proc Natl Acad Sci U S A* **112**:3698-3703.

Cai J, Damaraju VL, Groulx N, Mowles D, Peng Y, Robins MJ, Cass CE and Gros P (2008) Two distinct molecular mechanisms underlying cytarabine resistance in human leukemic cells. *Cancer Res* **68**:2349-2357.

Colca JR, McDonald WG, Waldon DJ, Leone JW, Lull JM, Bannow CA, Lund ET and Mathews WR (2004) Identification of a novel mitochondrial protein ("mitoNEET") cross-linked specifically by a thiazolidinedione photoprobe. *Am J Physiol Endocrinol Metab* **286**:E252-260.

Colmone A, Amorim M, Pontier AL, Wang S, Jablonski E and Sipkins DA (2008) Leukemic cells create bone marrow niches that disrupt the behavior of normal hematopoietic progenitor cells. *Science* **322**:1861-1865.

Coly PM, Gandolfo P, Castel H and Morin F (2017) The Autophagy Machinery: A New Player in Chemotactic Cell Migration. *Front Neurosci* **11**:78.

Crazzolara R, Bradstock KF and Bendall LJ (2009) RAD001 (Everolimus) induces autophagy in acute lymphoblastic leukemia. *Autophagy* **5**:727-728.

Eckert C, Henze G, Seeger K, Hagedorn N, Mann G, Panzer-Grumayer R, Peters C, Klingebiel T, Borkhardt A, Schrappe M, Schrauder A, Escherich G, Sramkova L, Niggli F, Hitzler J and von Stackelberg A (2013) Use of allogeneic hematopoietic stem-cell transplantation based on minimal residual disease response improves outcomes for children with relapsed acute lymphoblastic leukemia in the intermediate-risk group. *J Clin Oncol* **31**:2736-2742.

Fei F, Stoddart S, Muschen M, Kim YM, Groffen J and Heisterkamp N (2010) Development of resistance to dasatinib in Bcr/Abl-positive acute lymphoblastic leukemia. *Leukemia* **24**:813-820.

Fortney JE, Zhao W, Wenger SL and Gibson LF (2001) Bone marrow stromal cells regulate caspase 3 activity in leukemic cells during chemotherapy. *Leuk Res* **25**:901-907.

Fu X, Liu W, Huang Q, Wang Y, Li H and Xiong Y (2017) Targeting mitochondrial respiration selectively sensitizes pediatric acute lymphoblastic leukemia cell lines and patient samples to standard chemotherapy. *Am J Cancer Res* **7**:2395-2405.

Gati WP, Paterson AR, Larratt LM, Turner AR and Belch AR (1997) Sensitivity of acute leukemia cells to cytarabine is a correlate of cellular es nucleoside transporter site content measured by flow cytometry with SAENTA-fluorescein. *Blood* **90**:346-353.

Geldenhuys WJ, Funk MO, Awale PS, Lin L and Carroll RT (2011) A novel binding assay identifies high affinity ligands to the rosiglitazone binding site of mitoNEET. *Bioorg Med Chem Lett* **21**:5498-5501.

Geldenhuys WJ, Funk MO, Barnes KF and Carroll RT (2010) Structure-based design of a thiazolidinedione which targets the mitochondrial protein mitoNEET. *Bioorg Med Chem Lett* **20**:819-823.

Gomez AM, Martinez C, Gonzalez M, Luque A, Melen GJ, Martinez J, Hortelano S, Lassaletta A, Madero L and Ramirez M (2015) Chemokines and relapses in childhood acute lymphoblastic leukemia: A role in migration and in resistance to antileukemic drugs. *Blood Cells Mol Dis* **55**:220-227.

Hanahan D and Weinberg RA (2011) Hallmarks of cancer: the next generation. *Cell* **144**:646-674.

Holleman A, den Boer ML, Kazemier KM, Janka-Schaub GE and Pieters R (2003) Resistance to different classes of drugs is associated with impaired apoptosis in childhood acute lymphoblastic leukemia. *Blood* **102**:4541-4546.

Indran IR, Tufo G, Pervaiz S and Brenner C (2011) Recent advances in apoptosis, mitochondria and drug resistance in cancer cells. *Biochim Biophys Acta* **1807**:735-745.

Kakihara T, Fukuda T, Tanaka A, Emura I, Kishi K, Asami K and Uchiyama M (1998) Expression of deoxycytidine kinase (dCK) gene in leukemic cells in childhood: decreased expression of dCK gene in relapsed leukemia. *Leuk Lymphoma* **31**:405-409.

Kaspers GJ, Veerman AJ, Pieters R, Van Zantwijk CH, Smets LA, Van Wering ER and Van Der Does-Van Den Berg A (1997) In vitro cellular drug resistance and prognosis in newly diagnosed childhood acute lymphoblastic leukemia. *Blood* **90**:2723-2729.

Kimura T, Takabatake Y, Takahashi A and Isaka Y (2013) Chloroquine in cancer therapy: a double-edged sword of autophagy. *Cancer Res* **73**:3-7.

Klumper E, Pieters R, Veerman AJ, Huismans DR, Loonen AH, Hahlen K, Kaspers GJ, van Wering ER, Hartmann R and Henze G (1995) In vitro cellular drug resistance in children with relapsed/refractory acute lymphoblastic leukemia. *Blood* **86**:3861-3868.

Kuntz EM, Baquero P, Michie AM, Dunn K, Tardito S, Holyoake TL, Helgason GV and Gottlieb E (2017) Targeting mitochondrial oxidative phosphorylation eradicates therapy-resistant chronic myeloid leukemia stem cells. *Nat Med* **23**:1234-1240.

Laane E, Tamm KP, Buentke E, Ito K, Kharaziha P, Oscarsson J, Corcoran M, Bjorklund AC, Hultenby K, Lundin J, Heyman M, Soderhall S, Mazur J, Porwit A, Pandolfi PP, Zhivotovsky B, Panaretakis T and Grander D (2009) Cell death induced by dexamethasone in lymphoid leukemia is mediated through initiation of autophagy. *Cell Death Differ* **16**:1018-1029.

Lamba JK (2009) Genetic factors influencing cytarabine therapy. *Pharmacogenomics* **10**:1657-1674.

Lazarou M, Narendra DP, Jin SM, Tekle E, Banerjee S and Youle RJ (2013) PINK1 drives Parkin self-association and HECT-like E3 activity upstream of mitochondrial binding. *J Cell Biol* **200**:163-172.

Liliemark JO and Plunkett W (1986) Regulation of 1-beta-D-arabinofuranosylcytosine 5'-triphosphate accumulation in human leukemia cells by deoxycytidine 5'-triphosphate. *Cancer Res* **46**:1079-1083.

Mittler R, Darash-Yahana M, Sohn YS, Bai F, Song L, Cabantchik IZ, Jennings PA, Onuchic JN and Nechushtai R (2018) NEET Proteins: A New Link Between Iron Metabolism, Reactive Oxygen Species, and Cancer. *Antioxid Redox Signal*.

Mohle R, Schittenhelm M, Failenschmid C, Bautz F, Kratz-Albers K, Serve H, Brugger W and Kanz L (2000) Functional response of leukaemic blasts to stromal cell-derived factor-1 correlates with preferential expression of the chemokine receptor CXCR4 in acute myelomonocytic and lymphoblastic leukaemia. *Br J Haematol* **110**:563-572.

Moses BS, Evans R, Slone WL, Piktel D, Martinez I, Craig MD and Gibson LF (2016a) Bone Marrow Microenvironment Niche Regulates miR-221/222 in Acute Lymphoblastic Leukemia. *Mol Cancer Res* **14**:909-919.

Moses BS, Slone WL, Thomas P, Evans R, Piktel D, Angel PM, Walsh CM, Cantrell PS, Rellick SL, Martin KH, Simpkins JW and Gibson LF (2016b) Bone marrow microenvironment modulation of acute lymphoblastic leukemia phenotype. *Exp Hematol* **44**:50-59 e51-52.

Mudry RE, Fortney JE, York T, Hall BM and Gibson LF (2000) Stromal cells regulate survival of B-lineage leukemic cells during chemotherapy. *Blood* **96**:1926-1932.

Nair RR, Piktel D, Geldenhuys WJ and Gibson LF (2018) Combination of cabazitaxel and plicamycin induces cell death in drug resistant B-cell acute lymphoblastic leukemia. *Leuk Res* **72**:59-66.

Neri LM, Cani A, Martelli AM, Simioni C, Junghanss C, Tabellini G, Ricci F, Tazzari PL, Pagliaro P, McCubrey JA and Capitani S (2014) Targeting the PI3K/Akt/mTOR signaling pathway in B-precursor acute lymphoblastic leukemia and its therapeutic potential. *Leukemia* **28**:739-748.

Neuzil J, Dong LF, Rohlena J, Truksa J and Ralph SJ (2013) Classification of mitocans, anti-cancer drugs acting on mitochondria. *Mitochondrion* **13**:199-208.

Pedada KK, Zhou X, Jogiraju H, Carroll RT, Geldenhuys WJ, Lin L and Anderson DJ (2014) A quantitative LC-MS/MS method for determination of thiazolidinedione mitoNEET ligand NL-1 in mouse serum suitable for pharmacokinetic studies. *J Chromatogr B Analyt Technol Biomed Life Sci* **945-946**:141-146.

Pieters R, Huismans DR, Loonen AH, Hahlen K, van der Does-van den Berg A, van Wering ER and Veerman AJ (1991) Relation of cellular drug resistance to long-term clinical outcome in childhood acute lymphoblastic leukaemia. *Lancet* **338**:399-403.

Pogorzala M, Kubicka M, Rafinska B, Wysocki M and Styczynski J (2015) Drug-resistance Profile in Multiple-relapsed Childhood Acute Lymphoblastic Leukemia. *Anticancer Res* **35**:5667-5670.

Ristic B, Bosnjak M, Arsikin K, Mircic A, Suzin-Zivkovic V, Bogdanovic A, Perovic V, Martinovic T, Kravic-Stevovic T, Bumbasirevic V, Trajkovic V and Harhaji-Trajkovic L (2014) Idarubicin induces mTOR-dependent cytotoxic autophagy in leukemic cells. *Exp Cell Res* **326**:90-102.

Salem AF, Whitaker-Menezes D, Howell A, Sotgia F and Lisanti MP (2012) Mitochondrial biogenesis in epithelial cancer cells promotes breast cancer tumor growth and confers autophagy resistance. *Cell Cycle* **11**:4174-4180.

Schroder JK, Seidelmann M, Kirch HC, Seeber S and Schutte J (1998) Assessment of resistance induction to cytosine arabinoside following transfer and overexpression of the deoxycytidylate deaminase gene in vitro. *Leuk Res* **22**:619-624.

Slone WL, Moses BS, Evans R, Piktel D, Martin KH, Petros W, Craig M and Gibson LF (2016a) Modeling chemotherapy resistant leukemia in vitro. *J Vis Exp*:e53645.

Slone WL, Moses BS, Hare I, Evans R, Piktel D and Gibson LF (2016b) BCL6 modulation of acute lymphoblastic leukemia response to chemotherapy. *Oncotarget* **7**:23439-23453.

Sohn YS, Tamir S, Song L, Michaeli D, Matouk I, Conlan AR, Harir Y, Holt SH, Shulaev V, Paddock ML, Hochberg A, Cabanchick IZ, Onuchic JN, Jennings PA, Nechushtai R and Mittler R (2013) NAF-1 and mitoNEET are central to human breast cancer proliferation by maintaining mitochondrial homeostasis and promoting tumor growth. *Proc Natl Acad Sci U S A* **110**:14676-14681.

Stelzer G, Dalah I, Stein TI, Satanower Y, Rosen N, Nativ N, Oz-Levi D, Olender T, Belinky F, Bahir I, Krug H, Perco P, Mayer B, Kolker E, Safran M and Lancet D (2011) In-silico human genomics with GeneCards. *Hum Genomics* **5**:709-717.

Stow P, Key L, Chen X, Pan Q, Neale GA, Coustan-Smith E, Mullighan CG, Zhou Y, Pui CH and Campana D (2010) Clinical significance of low levels of minimal residual disease at the end of remission induction therapy in childhood acute lymphoblastic leukemia. *Blood* **115**:4657-4663.

Tamir S, Paddock ML, Darash-Yahana-Baram M, Holt SH, Sohn YS, Agranat L, Michaeli D, Stofleth JT, Lipper CH, Morcos F, Cabantchik IZ, Onuchic JN, Jennings PA, Mittler R and Nechushtai R (2015) Structure-function analysis of NEET proteins uncovers their role as key regulators of iron and ROS homeostasis in health and disease. *Biochim Biophys Acta* **1853**:1294-1315.

Zhang X, de Milito A, Olofsson MH, Gullbo J, D'Arcy P and Linder S (2015) Targeting Mitochondrial Function to Treat Quiescent Tumor Cells in Solid Tumors. *Int J Mol Sci* **16**:27313-27326.

Footnotes

Financial support: This work was supported by the National Institutes of Health National Institute of General Medicine [Grant U54GM104942, P20GM121322, P20GM103488, P20GM103434, S10OD016165, P20GM109098, P20RR016440]; and the Alexander B. Osborn Hematopoietic Malignancy and Transplantation Endowed Professorship.

Legends for figures

Figure 1. Structure of NL-1. The thiazolidinedione (TZD) warhead scaffold is shown in blue, alongside pioglitazone and rosiglitazone, which are classical TZDs.

Figure. 2. REH/Ara-C cell line is resistant to Ara-C. REH and REH/Ara-C were plated at 5 x 10^4 cells per well in a 96 well plate and treated with indicated doses of (A) Ara-C , (B) methotrexate (MTX) or (C) vincristine (VIN). The number of viable cells was analyzed following 72 hours of treatment. (D) The concentration-dependent curve was utilized to calculate the IC_{50} using CompuSyn software. All experiments were performed in triplicate at least three different times and the data is represented as mean ± SEM. * Ara-C treatment of the resistant REH/Ara-C cells did not induce cell death.

Figure 3. Characterization of the REH/Ara-C cell line. (A) REH and REH/Ara-C were plated at 5 x 10^4 cells per well in a 96 well plate and cell viability was analyzed every 24 hours for 4 days. (B) REH and REH/Ara-C cells were stained with flurochrome-conjugated antibodies targeting the different cell surface receptors. The intensity of the staining was acquired and analyzed using flow cytometry. (C) REH or REH/Ara-C cells were plated on the insert and allowed to migrate towards the bottom well containing no chemoattractant (media), 100 ng/ml SDF-1, bone marrow stromal cells (BMSC) or human osteoblasts (HOB). The number of migrated cells was counted using flow cytometry after 4 hours. (D) REH and REH/Ara-C cells were plated at 1 x 10^6 cells/ml for 24 hours and were then processed for RNA and subjected to realtime RT-PCR protocol as described in the method section. The $\Delta\Delta C_T$ were used to compare the fold change in expression of the indicated genes in REH/Ara-C cells compared to REH cells. All experiments were performed in triplicate

at least three different times and the data is represented as mean ± SEM. *, P<0.05, statistical significance as compared to REH cell numbers that migrated towards the BMSC at the end of 4 hours.

Figure 4. NL-1 decreases cell viability in ALL cell lines. ALL cell lines, (A) REH, REH/Ara-C and (C) NALM6, NALM1, SUPB15, TOM1, BV173 and JM1, were plated at 5 x 10^4 cells/well in a 96 well cell culture plate and treated with indicated concentrations of NL-1. The number of live cells was measured after 72 hours of treatment. (B & D) IC_{50} values were calculated from the concentration dependent curves of each cell line using the CompuSyn software. The data is represented as mean ± SEM of a study performed in triplicate and is a representative of experiments that were carried out at least three independent times.

Figure 5. NL-1 activity in hemosphere and chemotaxis assays. (A) SD1 cells were plated at 1 x 10^5 cells/well and allowed to form spheroids by culturing them for 4 days. Spheroid formation was confirmed by observation using light microscopy and then treated with 60 μM of NL-1 or PBS (V.C.) for 72 hours. At the end of treatment, the resulting hemosphere images were captured (A) and counted (B). (C) Number of viable SD-1 cells after treatment with NL-1 and expressed as the percent viability. (D) REH (C) or REH/Ara-C (D) were pretreated for 1 hour with either PBS (V.C.) or 60 μM of NL-1. After treatment the cells were plated on the insert and allowed to migrate towards the bottom well containing no chemoattractant (media), 100 ng/ml of SDF-1, bone marrow stromal cells (BMSC) or osteoblasts (HOB). The number of migrated cells was counted using flow cytometry after 4 hours. The data is represented as mean ± SEM and is a representative of experiments that were carried out at least three independent times. *, P<0.05, when compared to

V.C. treated group migrating towards media. #P<0.05 when compared to the V.C. treated group migrating toward SDF-1.

Figure 6. NL-1 induces cell death in co-culture through an autophagy dependent mechanism. REH and REH/Ara-C were grown in a co-culture with either bone marrow stromal cells (BMSC) or osteoblasts (HOB) in a 24 well plate for 12 days. On day 9 in co-culture, the cells were treated with 60 μM NL-1, CQ or vehicle/DMSO. At the end of treatment, the total live cells in suspension (S) and the leukemic cells buried under the adherent layer (PD) were counted using the trypan blue dye exclusion method (A & C). The total cells and the live cell population were used to calculate the % viability (B & D). *P<0.05, when compared to REH cells. (E) REH and REH/Ara-C cells were plated in a 96 well plate and selected wells were pre-treated for 1 hour with CQ. Following CQ treatment, the cells were treated with 60 μM NL-1. After 6 hours of treatment, the autophagic flux was measured. *P<0.05, when compared to REH control, #P<0.05, when compared to REH-Ara-C control group. (F) REH was plated at 5 x 10^4 cells per well in a 96 well plate and treated with indicated concentrations of CQ. Following 1 hour of CQ treatment the cells were exposed to 60 μM NL-1. After 72 hours of NL-1 treatment the cell viability was analyzed as described in the method section. *P<0.05, when compared to NL-1 REH treated group. #P<0.05, when compared to NL-1 REH/Ara-C treated group All data is presented as mean ± SEM and is a representative of a study performed in triplicate and conducted three independent times.

Figure 7. NL-1 does not affect primary immune cells but demonstrated anti-leukemic activity in a pilot *in vivo* study. (A) Normal primary B cells, T cells, peripheral blood mononuclear cells (PBMC) and bone marrow mononuclear cells (BMMC) were plated at 1 x 10^6 cells/ml in a

24 well plate and then treated with 60 μM NL-1 for 24 hours. The cells were then processed for flow cytometry using a Live/Dead stain following the manufacturer's instructions. (B) NSG female mice were injected with 1 x 10^6 luciferase expressing TOM-1 cells. Two days after engraftment the mice were treated with 10 mg/kg NL-1 for five days. The tumor burden was analyzed by IVIS imaging at the end of 14 days. All data were represented as mean ± SEM. *P<0.05, when compared to vehicle treated control (V.C.).

JPET Fast Forward. Published on April 22, 2019 as DOI: 10.1124/jpet.118.255984
This article has not been copyedited and formatted. The final version may differ from this version.

Figure 1

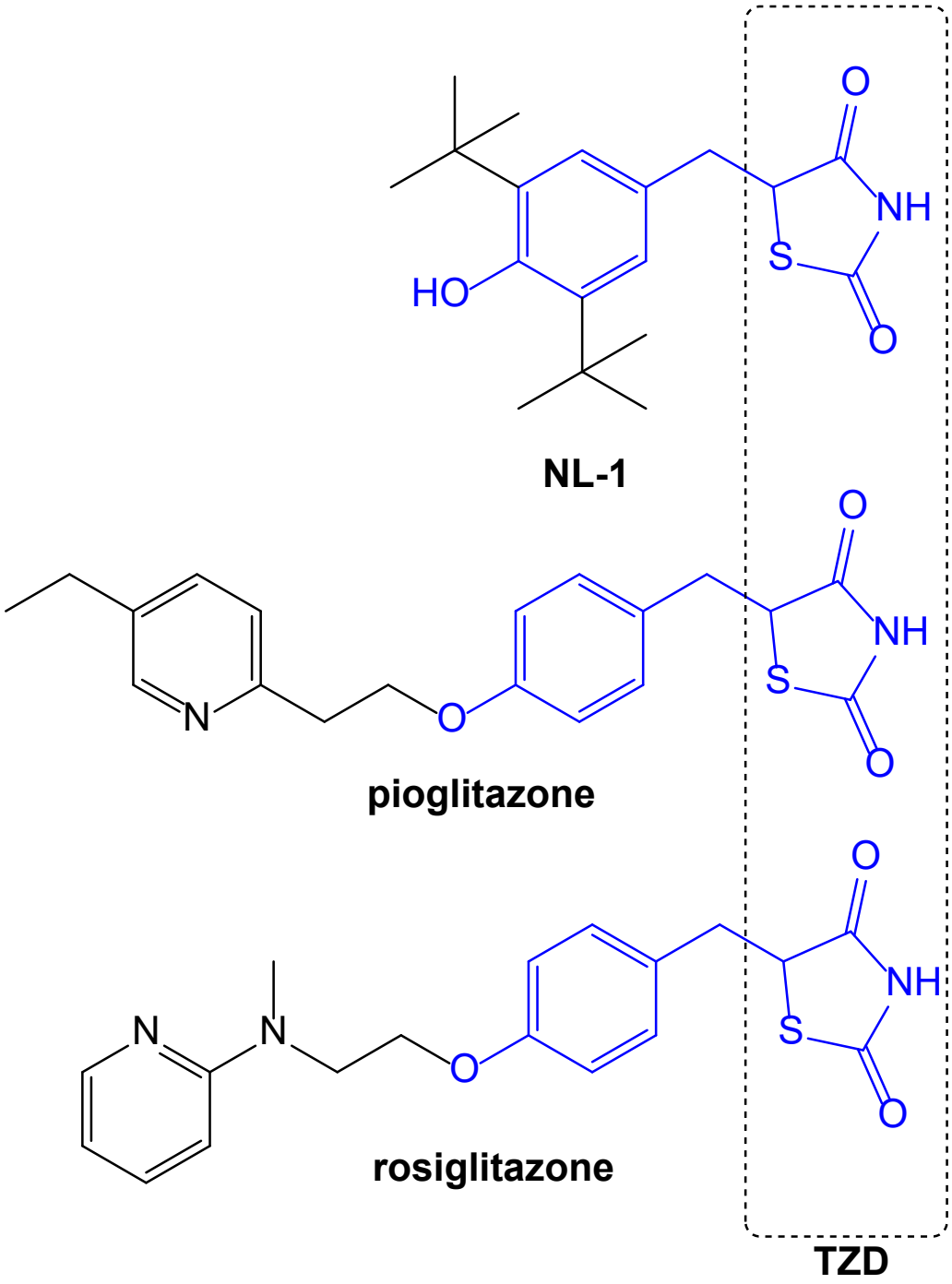

JPET Fast Forward. Published on April 22, 2019 as DOI: 10.1124/jpet.118.255984
This article has not been copyedited and formatted. The final version may differ from this version.

Figure 2.

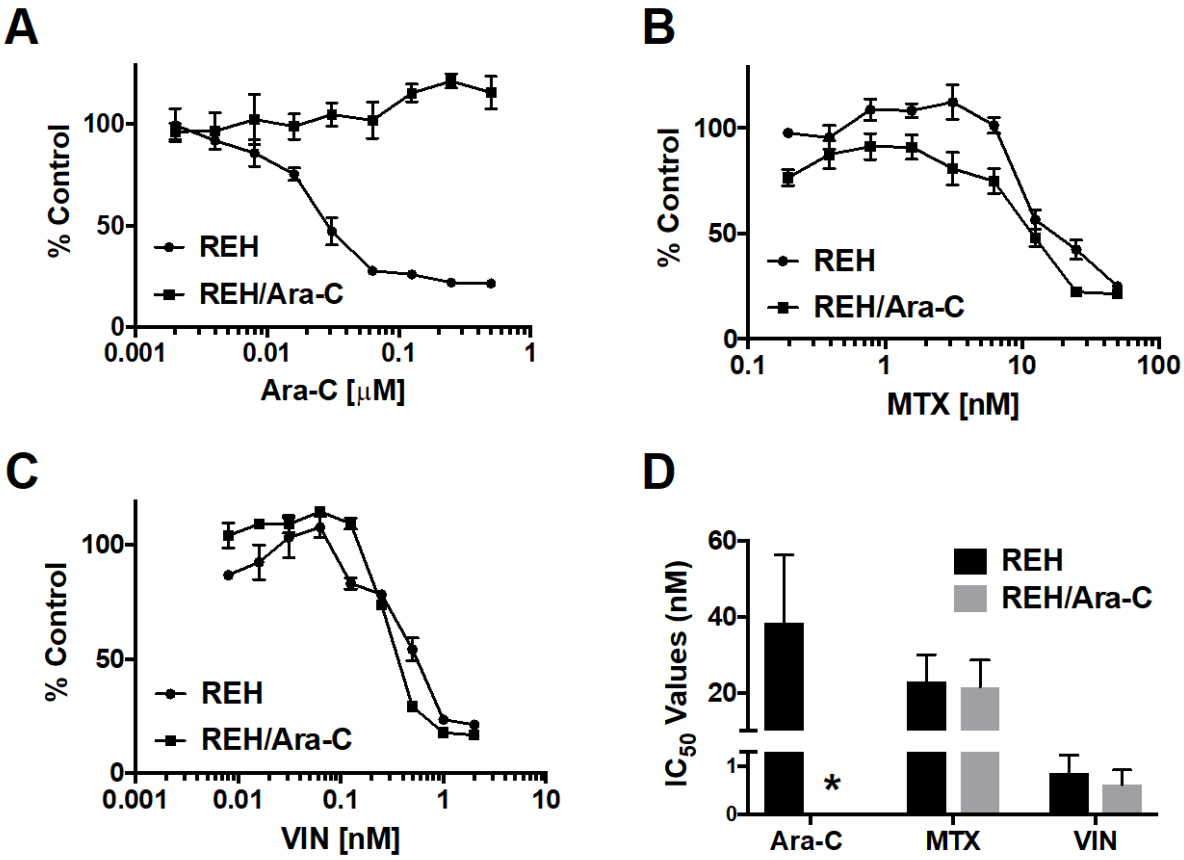

JPET Fast Forward. Published on April 22, 2019 as DOI: 10.1124/jpet.118.255984
This article has not been copyedited and formatted. The final version may differ from this version.

Figure 3.

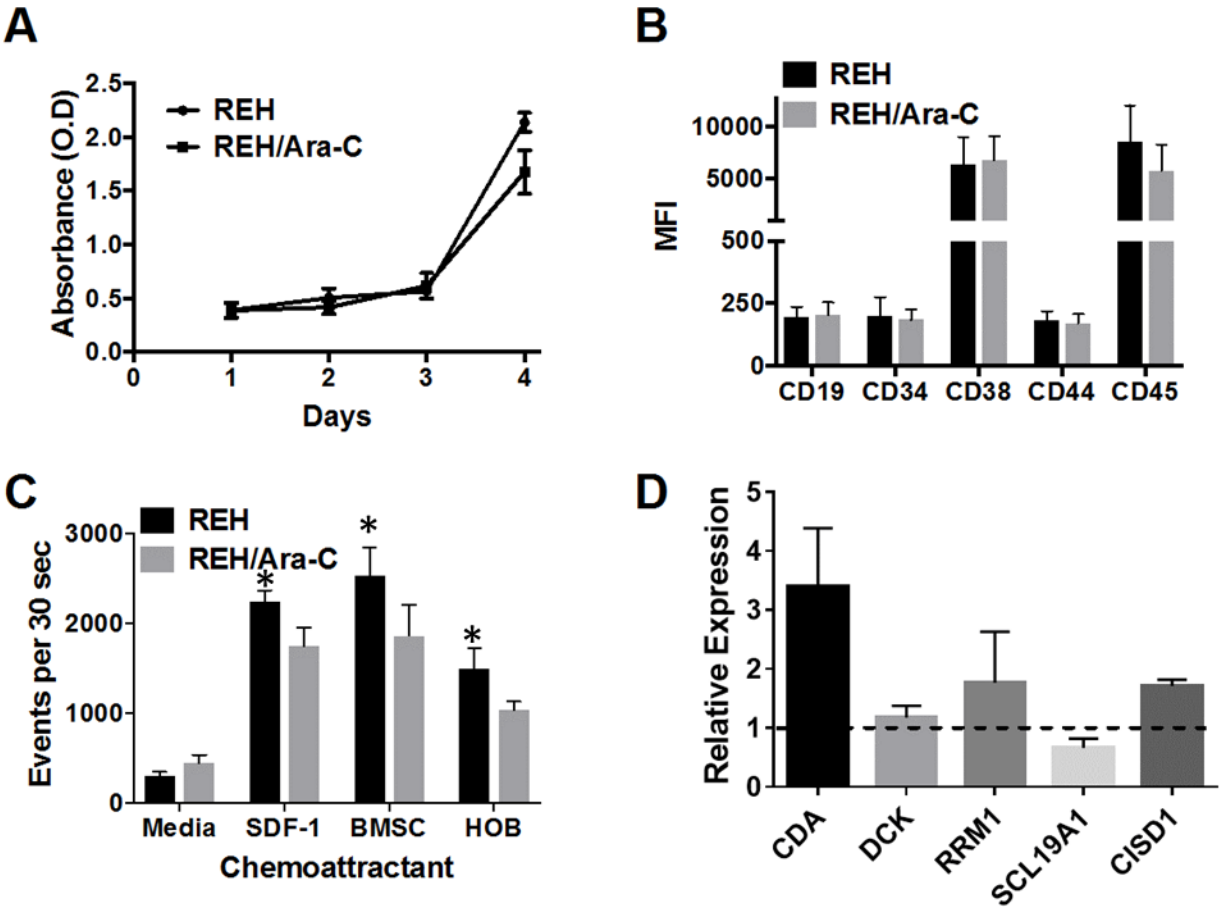

JPET Fast Forward. Published on April 22, 2019 as DOI: 10.1124/jpet.118.255984
This article has not been copyedited and formatted. The final version may differ from this version.

Figure 4.

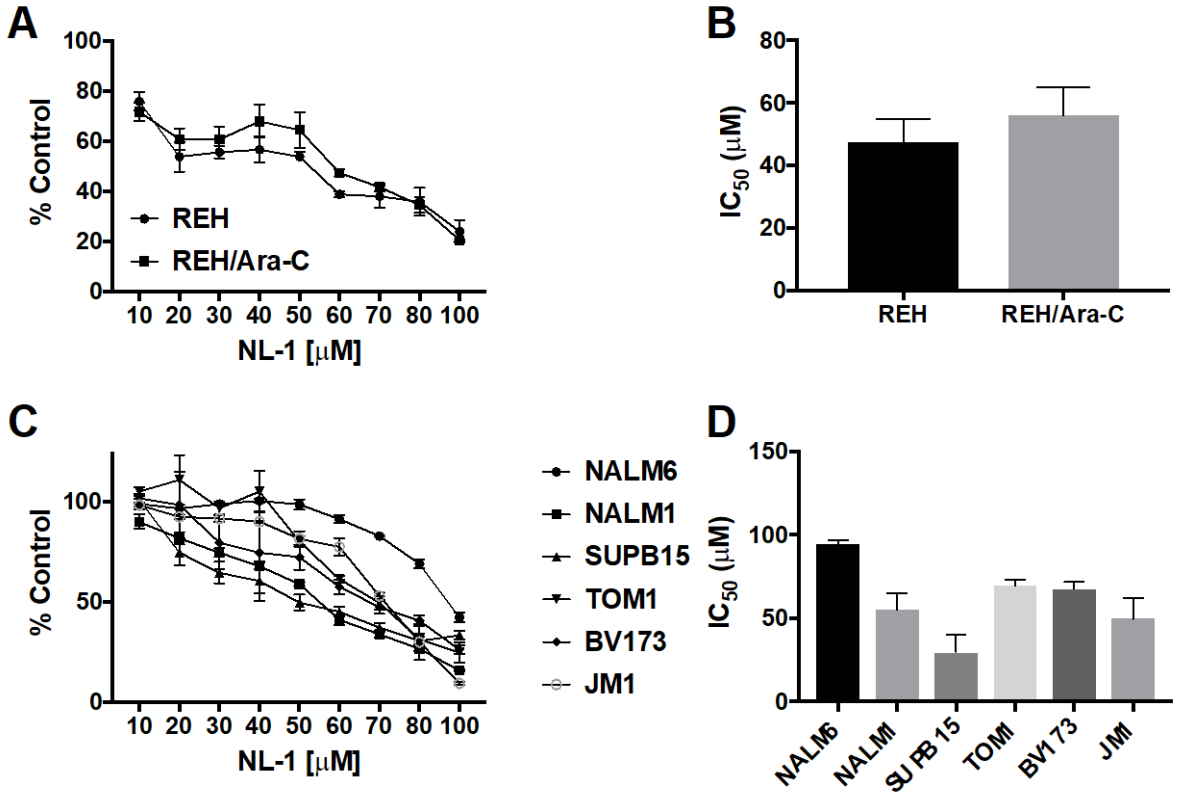

JPET Fast Forward. Published on April 22, 2019 as DOI: 10.1124/jpet.118.255984
This article has not been copyedited and formatted. The final version may differ from this version.

Figure 5.

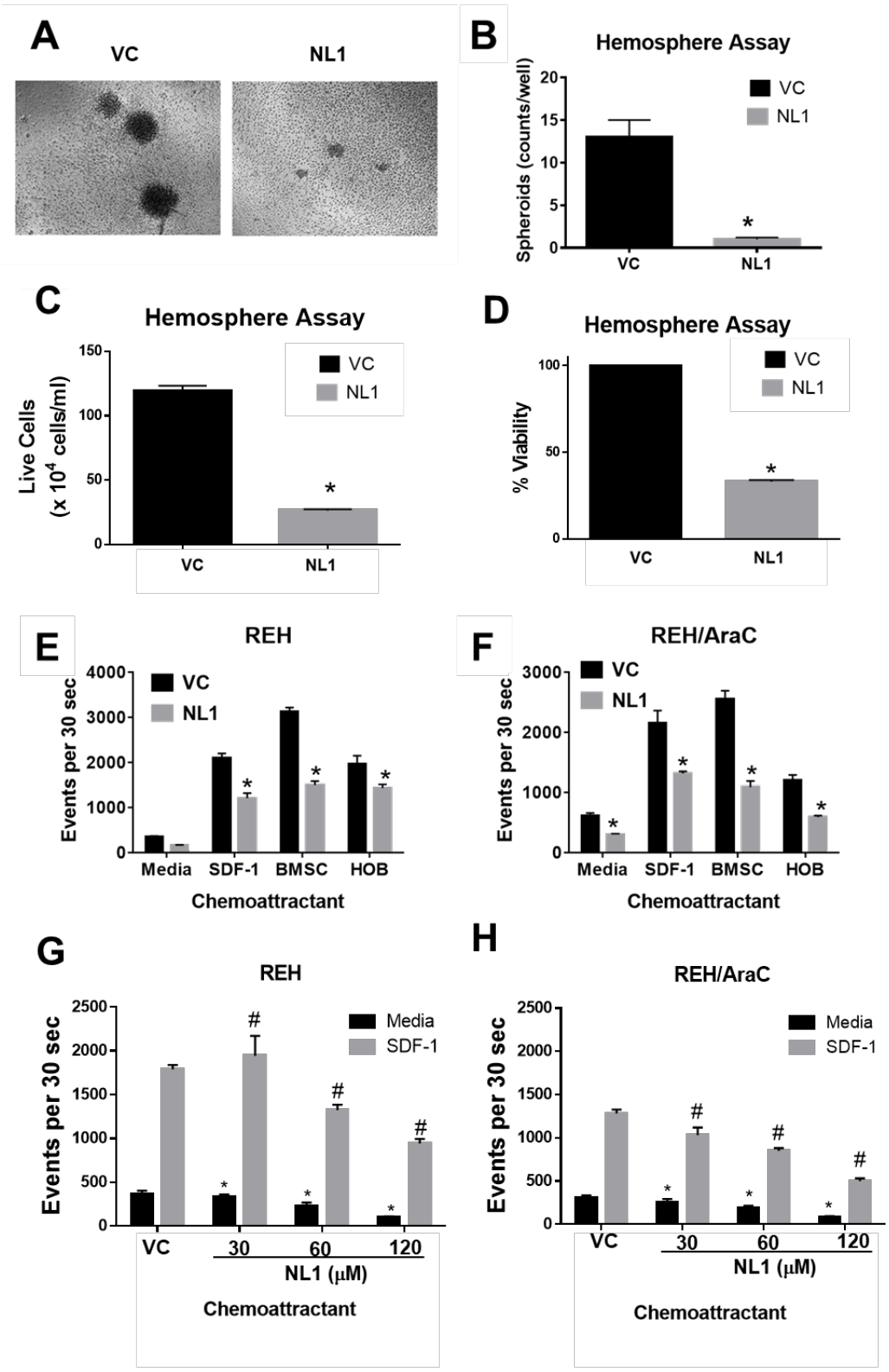

JPET Fast Forward. Published on April 22, 2019 as DOI: 10.1124/jpet.118.255984
This article has not been copyedited and formatted. The final version may differ from this version.

Figure 6.

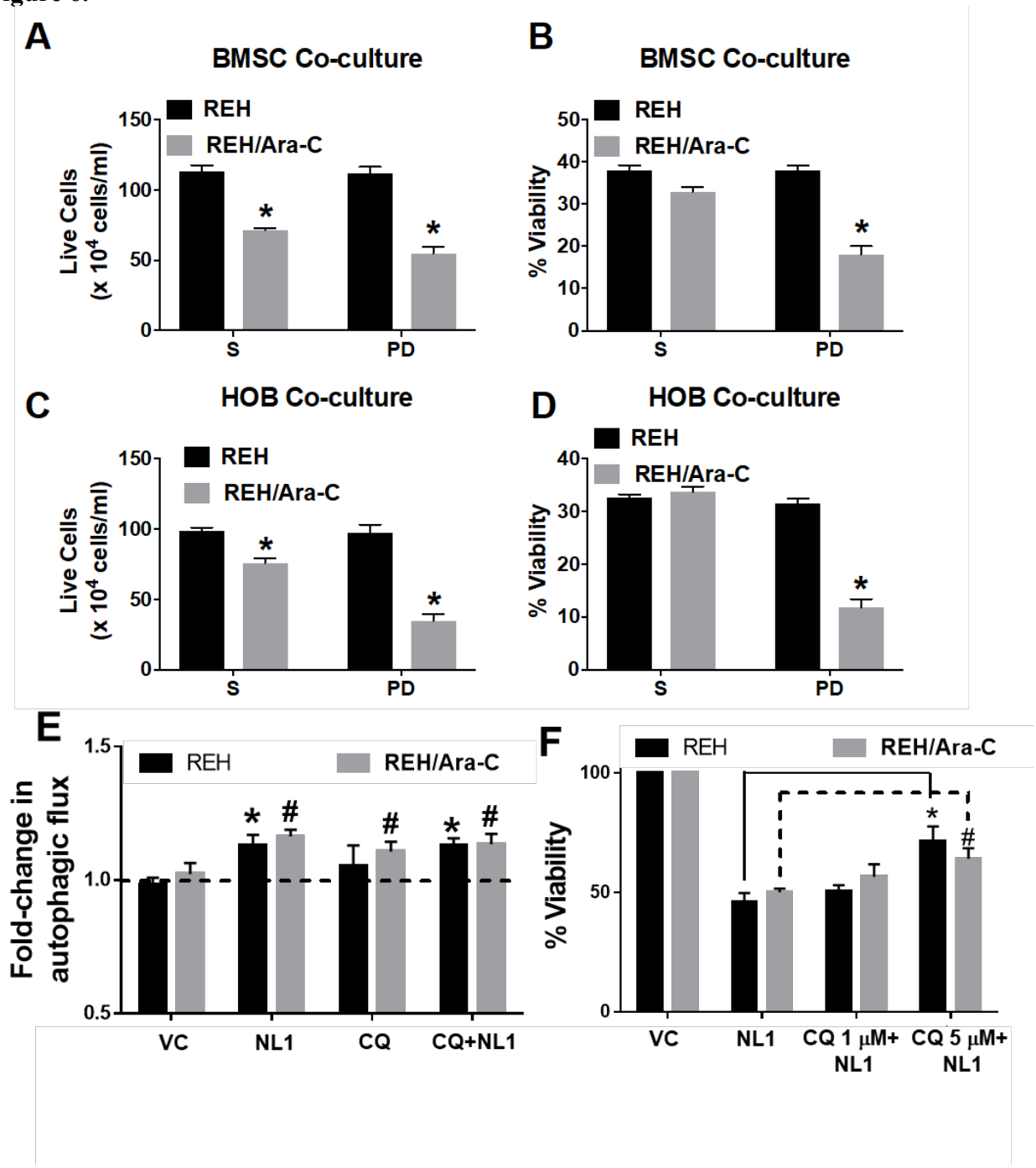

JPET Fast Forward. Published on April 22, 2019 as DOI: 10.1124/jpet.118.255984
This article has not been copyedited and formatted. The final version may differ from this version.

Figure 7.